ELECTRICAL BEHAVIOR DURING COOLING OF CONDUCTIVE CONCRETE

By

Mohamad Ali Alhakim

A thesis submitted to the faculty of
The University of North Carolina at Charlotte
in partial fulfillment of the requirements
for the degree of Master of Science in
Civil Engineering

Charlotte

2019

Approved by:

_____
Dr. Shen-En Chen

_____
Dr. Nicole Braxtan

_____
Dr. David Scott

ABSTRACT

MOHAMAD ALI ALHAKIM. Electrical Behavior During Cooling Of Conductive Concrete. (Under the direction of DR. SHEN-EN CHEN)

Self-sensing concrete consists of embedded conductive materials allowing enhanced electric conductivity for assessing mechanical properties. This thesis describes the design of a self-sensing concrete with steel fabrication waste and the detection of the electric responses during the cooling process from 115 °C. The thermal process is recorded using an infrared camera and the changes of the electric responses are correlated empirically. The thermal effect on the steel waste-modified concrete is the decrease in electric resistivity and to detect the change in resistivity, both voltage and current changes were investigated.

The electric field measurement for thermal property correlations involves multi-physical phenomenon and an attempt is made in describing the multiphysics in theoretical sense. Also investigated is the effect of temperature rising due to the continuous electric current flow through the material.

This study concludes that it is possible to correlate resistivity change to the thermal properties of the cooling concrete.

TABLE OF CONTENTS

LIST OF TABLES

LIST OF FIGURES

CHAPTER 1: INTRODUCTION

Deterioration and damage of concrete during its service period will lead to the loss of structural integrity and may cause an irreversible effect if not detected and handled in time, especially for critical structures. The American Society of Civil Engineers (ASCE) reports that almost four in ten bridges in the US are 50 years or older, and 9.1% of the nation's bridges were structurally deficient in 2016 (ASCE 2017). Nondestructive evaluation (NDE) is used to investigate and evaluate these structures, but the configuration and sensitivity of certain parts of the structures restrict the use of NDE. Therefore, it is necessary to have more accessible and continuous monitoring for the structural state to ensure the integrity of concrete structures.

To develop a viable monitoring technique, embedded sensors such as fiber-optic and continuous carbon fiber in cement have been used for damage sensing in concrete structures; however, these methods are expensive to implement and the installation process can be tedious. A better approach is to employ a measurement technique that can correlate to the bulk material properties. A less costly technique involves admixtures, which can be incorporated into the cement mix, has been suggested (Chung 2002).

In general, the use of structural materials as sensors without having embedded sensors is known as self-sensing (Chung 2002, Han et al. 2014). This technique is dependent on the blending of sensing-enabling additive materials into the concrete material and nano-carbon, steel slag, nickel, graphite, ceramic particles (piezoelectric effect, Oh et al. 2009), and others, have all been experimented (Rajabipour 2006, Wen and Chung, 2007)

Scott (2018) used recycled steel shavings (RSS), an industrial waste, as the functional additives to self-sensing concrete. The shavings are waste products from the steel fabrication processes and usually are either sent to steel production plants for making new steel or straight to landfill (Pace 2016). Figure 1 shows the typical form of the steel shavings waste. This enables the manufacturing of low cost and eco-friendly concrete. Several experiments have been performed and Scott (2018) concluded that 2% of clean steel shaving is the optimal percent for self-sensing concrete.

The principle behind self-sensing concrete is based on the appropriate modification of the concrete material properties such that the passing of electric currents through the material is enabled and the detection of the changes in the electric properties will allow the detection of material changes. The basic assumption is that internal changes in the concrete will affect its electric properties observed through the circulated current. This modified concrete is known as conductive concrete (Wu et al. 2013). In order to get a better correlation between the concrete material properties and the electrical properties, it is essential to understand all the material and environmental effects on the circulated current and the concrete electrical properties.

One of the major factors that affect the electrical flow and the response in the concrete is the thermal changes in the material (Guo et al. 2011). Most studies on thermal conductive concrete are in the areas of deicing (Yehia and Tuan 2000, 2002, Tuan 2004 and Yehia 2008) and concrete under extreme temperatures including climate effects (Videla et al. 1996). To get more reliable results from the self-sensing concrete, there is a need to discern the temperature effects on the electrical properties and current flow. This is the overall goal of this study.

In this thesis, the wasted steel shavings were used to make conductive concrete material as a low-cost solution for a large amount of concrete. The conductive concrete was subjected to evaluated temperature then the electrical response will be monitored during cooling. The thesis, herein, provides both experimental and numerical modeling using finite elements to verify the results. Figure 2 shows the setup for the forming of the conductive concrete including the electrodes for sensing.

FIGURE 1: Shaving wastes from steel fabrication process

FIGURE 2: Formwork for making self-sensing concrete

CHAPTER 2: ELECTRIC AND THERMAL RESPONSES OF CONDUCTIVE CONCRETE MATERIAL

Concrete is well known for its low thermal and electrical conductivities. The low thermal conductivity and high thermal mass of concrete inherently provide fire resistance and was the focus of many types of research to determine the behavior of concrete during fires and the use of special concrete mixes for structures exposed to extreme temperature or radiation exposure (Videla et al. 1996, Samarin 2013 and Wu et al. 2013, etc). The law of electrical conductivity of concrete, on the other hand, was a limiting factor for any attempt of circulating current in the concrete. The first to overcome this obstacle were Xie et al. (1996) and Yehia et al. (2000) by adding an electrically conductive component to the concrete mix to attain stable and high electrical conductivity. Conductive concrete allows the circulation of current to get the desired effect or to be able to detect the change in the material. Its potential applications include bridge and roadway deicing, anti-static flooring, and electromagnetic shielding (Yehia and Tuan 2000, 2002).

Within a self-sensing concrete, an electric measurement system is devised to help transmit and receive electric currents through the material. In most literatures reviewed, an alternative electric (AC) current is usually introduced into the material (Ou *et al*. 2009) – a technique described as active sensing. The selection of alternating current is critical for the success of resistivity detection, which is usually used as the indicator for property changes. The use of AC prevents the concrete element from becoming a capacitor and storing electricity within the concrete as in the direct current (DC) case.

To ascertain testing on large scale specimens, a low frequency (60 Hz) AC current is used. The low-frequency AC flow allows the electric current to penetrate deeper into the material and at the same time, eliminate the need for complex AC-AC conversion.

This study of electrical behavior during the thermal change will focus on two main areas, the temperature effect on electrical properties and the heat generated by the circulating current. The temperature rise will affect the electrical conductivity of the conductive concrete and the current flow.

According to Chung (2002) and Chrisp *et al*. (2001), conductive concrete has similar behavior as semiconductors that have a temperature-conductivity behavior governed by the Arrhenius equation:

$$\sigma = \alpha e^{\frac{-E_a}{kT}} \tag{1}$$

where σ is the electrical conductivity, α is a pre-exponential factor, E_a is the activation energy for the conduction process, k is the Boltzmann constant, and T is the absolute temperature in Kelvin. The natural logarithm of equation (1) gives the following equation:

$$\ln(\sigma) = \ln(\alpha) - \frac{E_a}{k}\left(\frac{1}{T}\right) \tag{2}$$

Alternatively, equation (2) can be rearranged and expressed as:

$$\ln(\sigma) = \ln(\alpha) + \frac{k}{E_a}\left(T\right) \tag{3}$$

Equation (3) indicates that the natural logarithm of conductivity is in direct relationship with the temperature. This implies that higher temperatures would allow the concrete to become more conducive for the current circulating through the concrete.

The heat generated by the applied current is one of the main concern in the electrical behavior during the cool-down study. Many research suggested using conductive concrete for bridge dicing by generating heat through the applied voltage (Yehia and Tuan 2000, 2002). Hence, a detail analysis for the affect of the heat generated on the cooling process is required. The heat generated by the applied current can be expressed by Joule's law, which is a physical law that gives the heat generated by the current flowing through a conductor:

$$H = I^2 R t \tag{4}$$

where H is the heat generated by a constant current (I) through a conductor having an electrical resistance (R) for a given time t. The current flowing in the conductor can be expressed by Ohm's first law as a function of the voltage applied V and the conductor resistance R:

$$I = \frac{V}{R} \tag{5}$$

The electrical conductivity of the concrete is inversely proptional to the resistance (from Ohm's second law) and the resistance R of a conductor with electrical conductivity σ along an internal electrical distance of L and electrode conductive area A is:

$$R = \frac{L}{\sigma A} \tag{6}$$

Substituting Eq. (5) into the Joule's law we can get:

$$H = \frac{t V^2}{R} \tag{7}$$

The heat H is the thermal energy that can cause a temperature change, ΔT, in a substance:

$$H = m\, C_p\, \Delta T \tag{8}$$

where m is the mass of the substance with a specific heat of C_p.

The rise of temperature in the conductive concrete due to the circulated current can be obtained by substituting Eq. (8) in Eq. (7) and is expressed as:

$$\Delta T = \frac{t\, V^2}{R\, m\, C_p} \tag{9}$$

CHAPTER 3: CONDUCTIVE CONCRETE MIX DESIGN

The conductive concrete considered in this project is prepared by adding recycled steel shavings (RSS) to the concrete mix to attain high electrical conductivity. Mixture proportioning and concentrations of recycled steel shavings were developed according to ACI 211 (2014) and ACI 544 (2018). The addition of steel shavings can increase the compressive strength because steel fibers randomly distributed in the matrix behave as crack resistor by bridging mechanism. To help prevent a reduction in workability and maintain consistency, two types of admixtures were used to reduce the likelihood of slump loss – water reducer (WR, Type A) and high-range water reducer (HRWR, Type F). Additionally, the steel shavings were sieved to better characterize their aspect ratio and to facilitate workability. For this project, the coarse aggregate (CA) and fine aggregate (FA) were reduced according to the corresponding volume of added steel, and they were measured to achieve an approximate FA-to-CA ratio of one (Scott 2018). The reduction in coarse and fine aggregates was approximately equivalent, by volume. The concrete was mixed according to ASTM C94 and ASTM C192.

Three mixture designs were developed corresponded with recycled-steel-residual (RSR) ratios of 0%, 1%, and 2% relative to bulk volume. Table 1 indicates the concrete mixtures used for the column testing of this project and the theoretical plastic properties and mixture designations.

TABLE 1: Concrete mixtures

Mixture Component/Parameter	**0.0% RSS**	**1.0% RSS**	**2.0% RSS**
Cement, kg.	44.45	44.45	44.45
Water, kg.	18.82	18.82	18.82
Coarse aggregate, kg.	107.18	104.14	101.10
Fine aggregate, kg.	112.49	109.22	106.15
Recycled steel residuals, kg. (Retained on No. 8 sieve)	0.0	3.11	6.21
Recycled steel residuals, kg. (Passing through No. 8 sieve)	0.0	6.21	12.38
Water-reducer (Type A), mL (oz. per 100 wt.)	86.8 (2.9)	86.8 (2.9)	86.8 (2.9)
Water-reducer (Type F), mL (oz. per 100 wt.)	34.7 (1.2)	34.7 (1.2)	34.7 (1.2)
Theoretical plastic density, kg/m^3	2378.74	2430.00	2482.86
w-cm ratio	0.45	0.45	0.45
RSR ratio by volume of mixture, %	0	1.0	2.0
Fine-to-coarse aggregate ratio	1.03	1.03	1.03

Testing for plastic properties includings unit weight (ASTM C138, 2001), slump (ASTM C143, 2003), air content (ASTM C231, 2004), and temperature (ASTM C1064, 2004) was performed made for each mixture as recorded in Table 2.

TABLE 2: Concrete plastic properties

Plastic Property	**0.0% RSS**	**1.0% RSS**	**2.0% RSS**
Unit weight, kg/m3	2340	2105	2005
Slump, mm	100	150	82.5
Air content, %	3	15	20
Temperature ˚C	18.3	19.4	17.8

For the cooling tests, columns were made with dimensions of 150x150x500 mm. Figure 3 shows the form work for making the conductive concrete with the electrode placements. Figure 4 shows the schematic for the electrode embedments, which dictates the direction of the electric current flow and measurements.

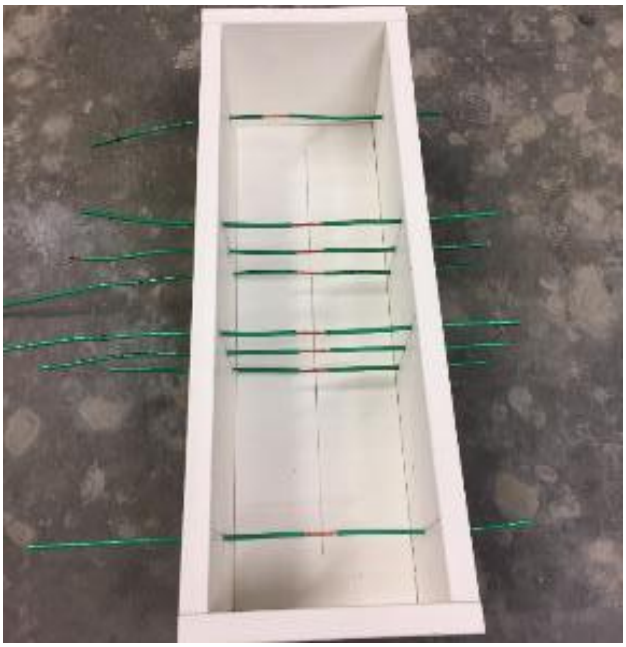

FIGURE 3: Electrodes placement through the column

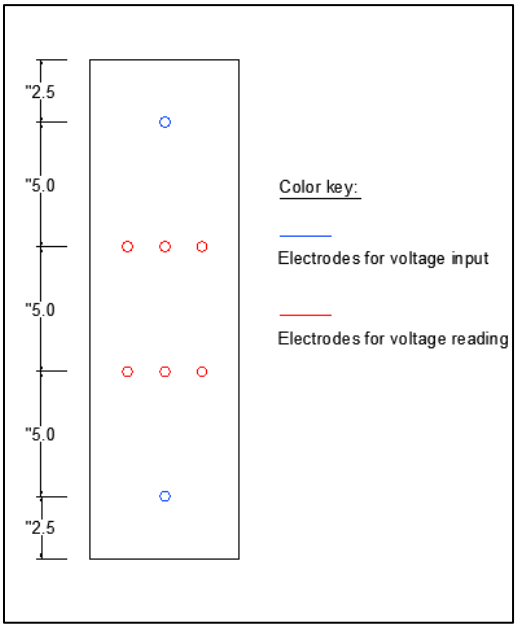

FIGURE 4 The Measurement scheme with embedded electrodes for both measurements and inducing electric current

CHAPTER 4: COOLING TESTS

In this test, the concrete specimens were placed in an oven and subjected to high heat until the concrete reached uniform temperature of 115^{o}C. The specimens were then retrieved from the oven and allowed to cool down to room temperature while voltage was applied through an AC power supply. Changes to the electrical flow were observed and recorded during this process.

To prevent polarization of the concrete, alternating current (AC) was imparted into the concrete (Rajabipour 2006). The current was applied with a 25.5-Volts from an AC power transformer through embedded electrodes located at 62.5 mm from the ends of the concrete column. The electrical outputs were taken from three pairs of embedded electrodes spaced at 125 mm. Electrode placement in the concrete columns is shown in Figure 4. Electrodes consist of 10 Ga., stranded copper with 24-mil insulation. The insulated wires were placed through the forms before casting the concrete, and the wire insulation stripped at the location where the electrical response was measured (Figure 4). The length of the electrodes protruding through the wires was equivalent, and the exposed length of wire was one inch.

Three cured concrete columns with 0%, 1%, and 2% RSS were placed in a lab oven at a temperature of 115˚C (240˚F) for 48 hours. After attaining a uniform temperature of 115˚C through the concrete, the columns were taken out of the oven and cooled to a room temperature of 23˚C (73.5˚F). Temperature measurements were tracked and recorded using an infrared camera.

At the start of the cooling process, the current data acquisition device was connected to the three pairs of inner electrodes, and the power source was connected to the outer electrodes to create a current circuit (Figure 5).

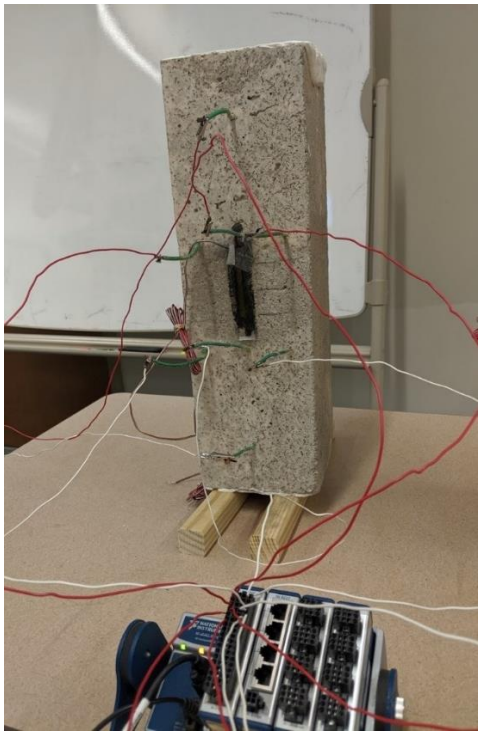

FIGURE 5 Data acquisition and current connections

The voltage measurements were recorded using a National Instrument (NI) data logger (NI 9205) with analog input module with three parallel differential channels at a sampling rate of 1000 S/s, and with a maximum voltage reading of 10 V. The voltage reading was taken at 10˚C temperature intervals from 110˚C to 40˚C. The durations of each test were greater than three hours. The cooling tests for voltage was conducted three times and the average of three three tests data were used.

A current test was required to study the resistivity of the concrete. A later test was performed and the current readings were recorded using the same device and sample rating with a maximum current reading of 0.04 amperes, and a temperature range of 70˚C to 40˚C.

The infrared camera recorded the surface temperature of the concrete column, the side faces of the columns were used to eliminate the interference from the electrodes. To validate the measurements, the inner temperature at the exposed electrodes were verified using a finite element 3-D transient heat transfer model.

CHAPTER 5: FINITE ELEMENT SIMULATION

A 3-D transient heat transfer model was developed using ABAQUS finite element software. The cooling process was simulated in order to confirm the relation between the inner temperatures of the concrete columns at the exposed electrodes and the recorded surface temperature.

A validation study was first conducted to verify the boundary condition and the conductive concrete thermal parameters used in the test. The validation check was made by comparing the time required to reach 40° C surface temperature in the model with the time recorded in the cooling test.

Three models were constructed for 0%, 1%, and 2% recycled steel residuals content in the columns. For different models, the thermal properties and boundary conditions were assumed the same with the exception of concrete density that is affected by the air content in the columns. All the units in the finite element model were inputted in the SI unit system.

The 150x150x500 mm concrete column was modeled as a single 3D component. The concrete thermal conductivity and specific heat were obtained from Eurocode 2 (EN 1992-1-2, 2004) as temperature-dependent variables. Table 3 shows the thermal properties used at different temperatures.

TABLE 3: Concrete thermal properties used in the FEM model

T (°C)	Conductivity k_c (W/m-K)	Specific Heat C_p (J/kg-K)	Density 0% RSS (kg/m^3)	Density 1% RSS (kg/m^3)	Density 2% RSS (kg/m^3)
20	1.95	900	2340	2105	2005
50	1.88	900	2340	2105	2005
80	1.81	900	2340	2105	2005
115	1.73	915	2340	2105	2005

Three models were constructed for 0%, 1%, and 2% recycled steel residuals content in the columns. For different models, the thermal properties and boundary conditions were assumed the same with the exception of concrete density that is affected by the air content in the columns All the units in the finite element model were inputted in the SI unit system.

Automatic incrementation was specified for the transient heat transfer analysis, with time increments limited by a minimum of one and maximum of five minutes and a maximum temperature change of 5° C. The column initial temperature was specified with a predefined field magnitude of 115° C and the ambient temperature was set at 23° C.

Concrete boundary conditions were assumed according to Eurocode and other research (*Lixia, Nagy*), then it was confirmed in the validation check of the base model with no steel shavings. The surface film coefficient for convection was assumed as 6 (W/M-K) with no radiation.

For more accuracy in the reading, the column was divided into small 25 mm cubes that are defined as 3D 8-node linear isoparametric element (Figure 6). The temperature in the surface central nod and the half-section central node were reported.

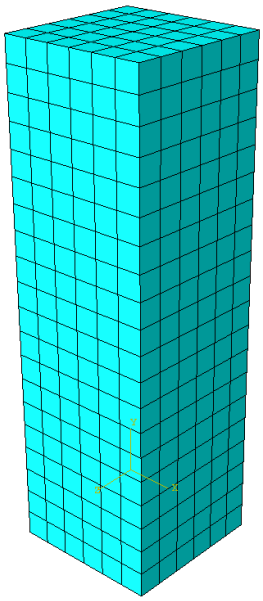

FIGURE 6 Finite element model

CHAPTER 6: RESULTS AND DISCUSSION

6.1 Voltage-Current Relationship

To investigate the change in electric resistivity, measurements in voltage and current were performed. The electric current reading for all specimens of different steel shaving contents are shown in Figure 7. The voltage drop reading for all specimens of different steel shaving contents are done separate from the current reading and is presented in Figure 8. The current data were obtained from one cooling test between a temperature of 70°C and room temperature with a constant applied voltage of 25.5 V from the AC tranformer. The voltage was applied over 375 mm of concrete, and the readings were taken at a distance of 125 mm with 125 mm space between the voltage input and the reading electrodes from each side. The change in the voltage readings was due to concrete resistance between the electric input location and the location where the data was acquired. The concrete can be represented as three electrical resistors in series. A resistance between the voltage input and the first electrodes row, a resistance between the first and second electrodes rows, and resistance between the second electrodes row and the voltage output.

The current and voltage readings for the 1% and 2% specimens follow the same trend, both of them decrease with the decrease in temperature. The current on the 0% specimens shows the same trend as the voltage before 40°C with a little deviation between 40°C and room temperature. Following Ohm's first law (R=V/I), the concrete resistance increased by 6% between 70°C and 23°C for the 1% specimen and increased by 7% for the 2% specimen. The 0% specimen resistance did not have any change until 40°C but decreased by 5% from 40°C and 23°C. According to E*quation 6*, the resistance is inversely

proportional to the concrete conductivity. Hence, we can confirm that in the specimens with steel shavings, the electrical conductivity is proportional to the concrete temperature.

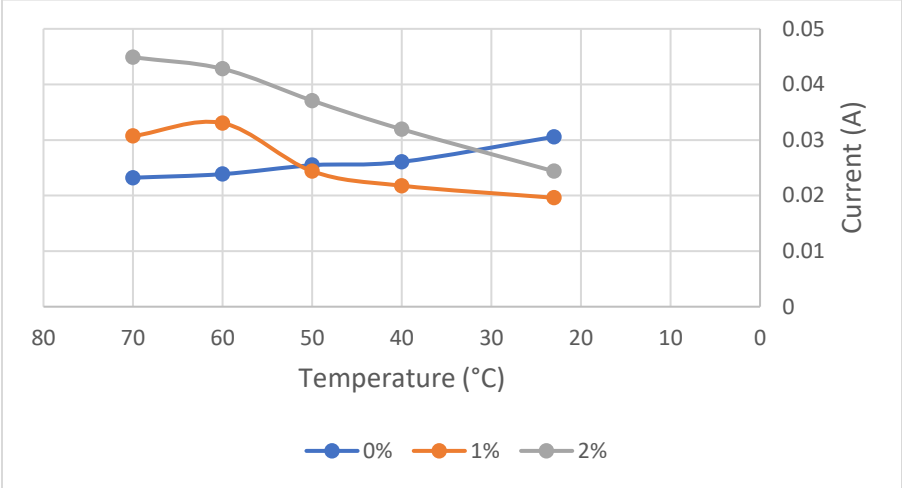

FIGURE 7 Current test: current vs temperature

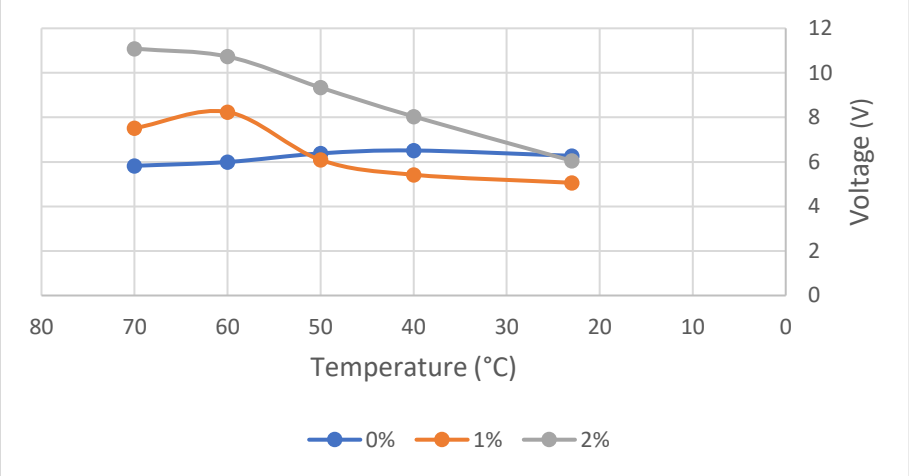

FIGURE 8 Current test: voltage vs temperature

6.2 Voltage-Temperature Relationship

The average voltage and temperature readings for the three cooling tests are given in Figure 9. It is shown that the voltage decreased with the temperature drop. Specifically, the voltage decreased by around 4 volts from the temperature of 110°C to 40°.

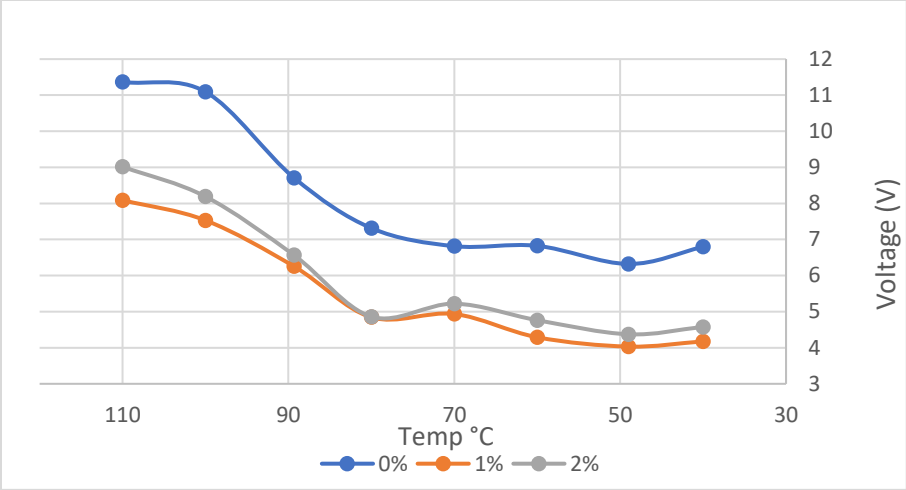

FIGURE 9 Voltage test: voltage vs temperature

The voltages reading for the 0% specimen were higher than the voltage readings for the 1% and 2% specimens. The higher voltage value is due to a higher resistance in the concrete without steel shavings.

Even though the total voltage drop was not affected by adding 1% or 2% of steel shavings in the column, the specimen without steel shavings did show a different behavior when compared to the specimen with shavings. We will look at the responses of specimen with steel shavings closely:

Careful examining Figure 9 indicates that the voltage curve has a steep decrease at a temperature around 80°C, after which the curve slope became gradually level. This observation is consistent for all the experiments performed on the specimens with steel shavings. In order to better describe the trendlines, the curves are separated and modeled separately at 80°C. Using trendline analysis for the correlation coefficients between the voltage and temperature between 110°C and 80°C is 0.99 for the 1% and 2% specimens, and is 0.97 for the 0% specimen, which corresponds to a linear relationship. However, the linear behavior deviates after 80°C for the 1 and 2% specimens the voltage slightly

increases between 80°C and 70°C and all the specimens show a slight increase in voltage after 50°C. The normalized voltage and temperature against time are shown in Figure 6, with a gap after 80° to separate the linear and non-linear sections.

The decrease in the voltage is mainly related to the change in the electrical conductivity of the concrete. With higher temperatures, the electrical conductivity will increase resulting in higher current and voltage in the concrete. The electrical conductivity has high sensitivity to the temperature change between 80°C and 110°C and becomes less sensitive as the temperature decreases.

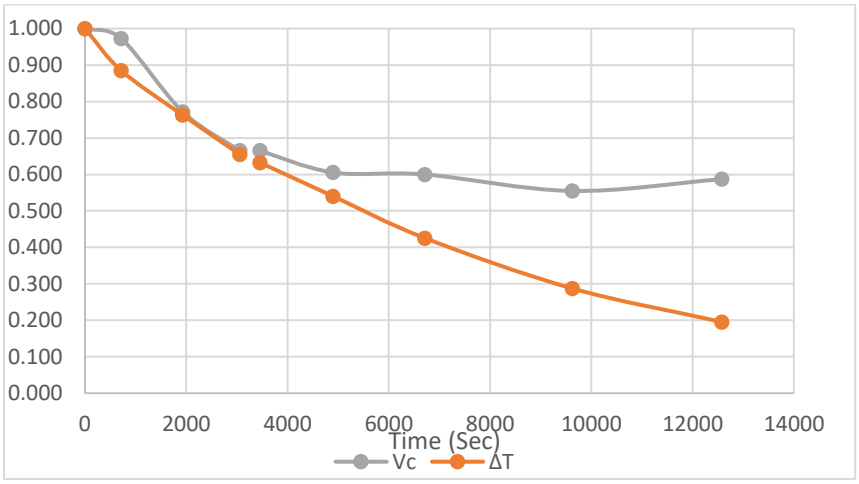

FIGURE 10 (a) Normalized temperature and voltage (0%)

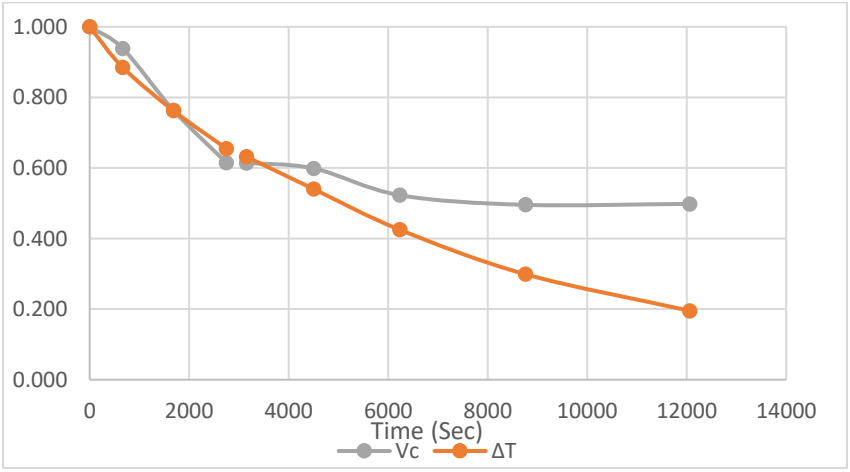

FIGURE 10 (b) Normalized temperature and voltage (1%)

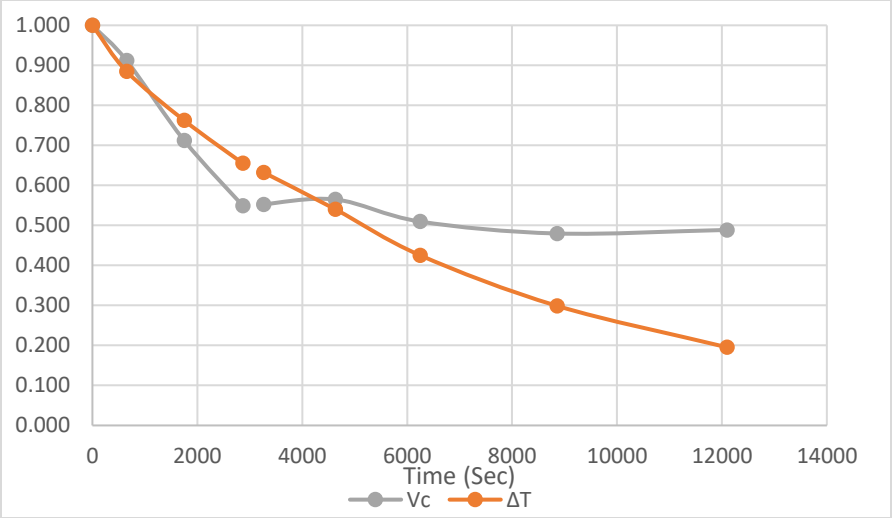

FIGURE 10 (c) Normalized temperature and voltage (2%)

The rise in temperature between 80°C and 70°C in the 1% and 2% specimen can be traced back to an increase in concrete conductivity at that temperature. Figure 5 and Figure 6 inducate that higher steel shavings contents resulted in an increase in voltage at that range, while the 0% specimen did not have any voltage increase. This indicates that the steel shavings slightly increase the concrete conductivity at this range.

The temperature drop time is related to the difference in temperature between the specimen temperature and room temperature. Higher temperatures with higher difference with room temperature correspond to a faster cooling time. The specimen takes 11 minutes to cool down from 110°C to 100°C, while it takes 53 minutes to reach 40°C from 50°C. The longer the time needed to reach the next temperature, the longer the flowing of the current inside the concrete. While the effect of longer exposure of the AC current in the concrete is minimum it still can have some effects on the last few readings.

6.3 Temperature Generated by Voltage

According to *Equation (9)*, the temperature increase due to the heat generated by the current is proportional to the duration of the applied voltage and the amount of voltage applied to the system, and it is inversely proportional to the resistance of the system, the mass of the concrete between that is resisting the current, and the specific heat of the concrete. To determine the effect of heat generation due to electric current through the conductive concrete, a calculation of the temperature generated is done for the 2% specimen.

The heat generated is calculated for the 375 mm distance between the voltage input and output where the voltage applied is 25.5 volts (V). The mass of the concrete is assumed constant throughout the test, which is determined by multiplying the cross-section area of the column by the length that is resisting the current and by the density of the concrete. The concrete density of the concrete is 2005 kg/m^3 (Table 2), the length of the resistance is equal to 0.381 meters. The cross section of the column is 150 mm by 500 mm (0.077 m^2). The mass of the concrete is calculated in as:

$$m = \sigma . L . A = 2005x\ 0.381x\ 0.077 = 59.14\ kg \quad (10)$$

The specific heat will be assumed constant through the test, from *Table 3* the specific heat is 900 J/kg-K. The resistance will be taken as the lower resistance calculated in the first test to maximize the heat generated, which equals to 205 ohms (Ω) for 125 mm of concrete. The total resistance will be three times the calculated resistance in the first test for a total of 615 Ω. The total time of the test was 3 houres and 14 minutes (11,640 seconds). Inputing all the variables in equation (9) the total temperature generated in the test is only 0.23°C.

The low temperature is due to the low voltage used. It should be noted that in research works related to heat generation for the purpose of deicing, a voltage value of 220 V to 400 V were typically used.

6.4 Finite Element Modeling

The purpose of the finite element modeling is to validate the cooling process of the concrete column and study the interior temperature of the specimens. Table 4 shows the time required for the temperature to drop from 110˚C to 40˚C. The experimental thermal changes were obtained by using an infrared camera that showed the surface temperature of the concrete columns, the duration of the three tests for 0%, 1%, and 2% specimens are recorded along with the thermal imaging. The finite element data are the outputs of the three models with the difference in the concrete density. The concrete densities used are the same densities of the 0%, 1%, and 2% specimen recorded in Table 2.

TABLE 4: Time required for the surface temperature to reach 40˚in hours:minutes

	0% RSS	1% RSS	2% RSS
Test results	3:30	3:20	3:14
Finite Element - Surface	3:36	3:15	3:10
Finite Element - Center	4:00	3:35	3:25

From Table 4 it is noted that the cooling time is shorter for the specimens with steel shavings, with the 2% RSS mix reaching the 40 ˚C 16 minutes faster than the 0%. From the finite element modeling results, we can conclude that the main reason for the cooling time difference is the change in density. The density change is a result of the higher air voids ratio in the specimens with the steel shavings.

Figure 11 shows the temperature-time relationship for the surface face of the test specimen and both the surface and the interior section of the finite element models. From Figure 5 and Table 4 indicate that the interior section temperature drop has the same behavior as the surface temperature with a temperature difference not exceeding 5 ˚C. The interior takes more time to reach 40 ˚C because the temperature drop will slow down when it is close to the room temperature. The interior temperature in the 2% specimen has the least difference with the surface temperature, this can again be related to the higher air voids contant that allow easier conduction in the specimen. Figure 12 shows the interior temperature when the surface central temperature reached 40 ˚C.

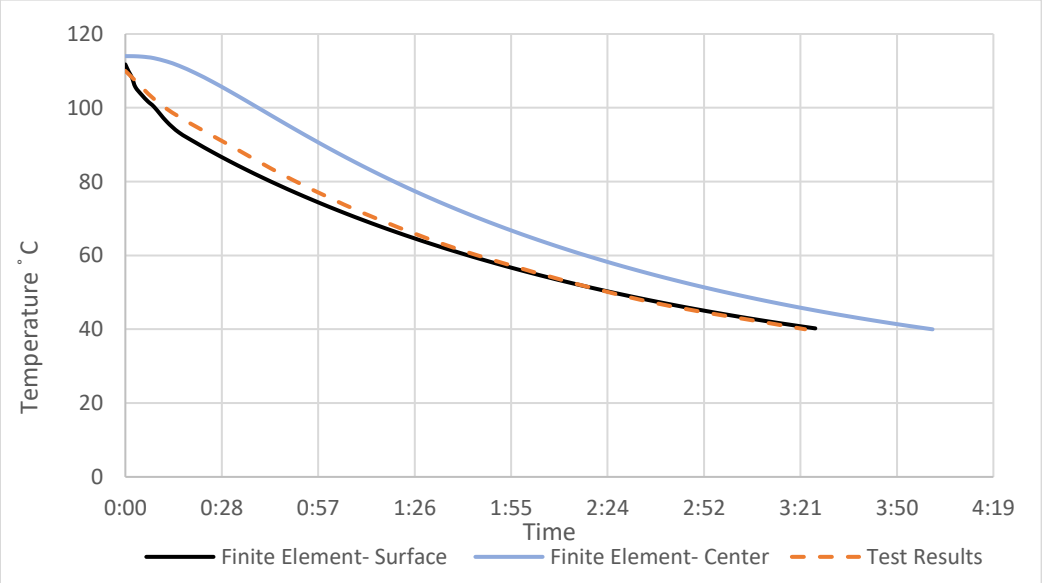

FIGURE 11 Temperature-time relationship (0% concrete)

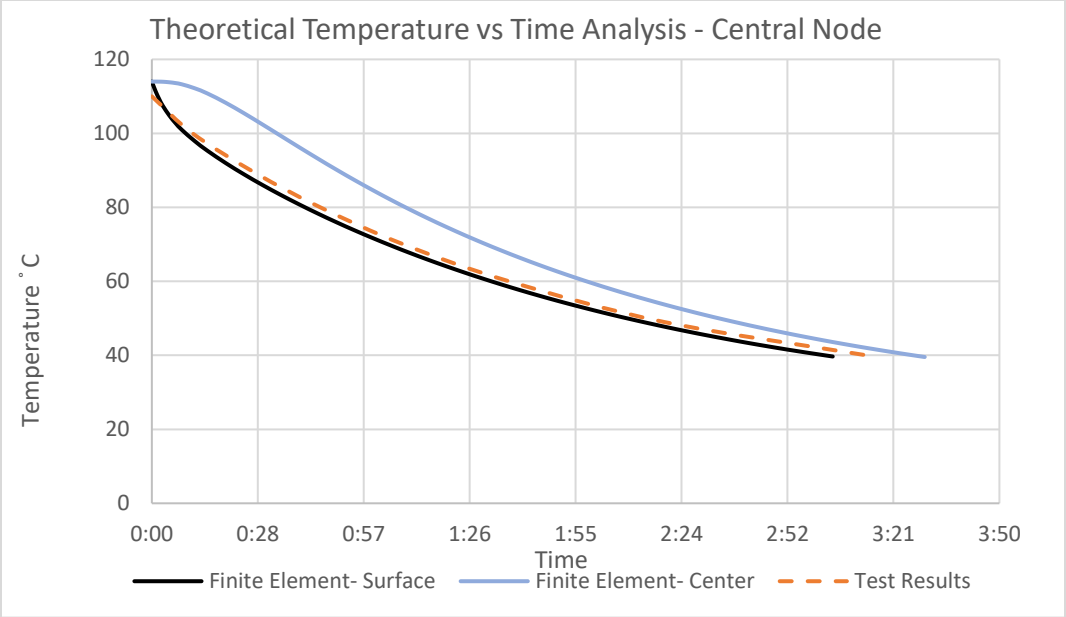

FIGURE 11 (b) Temperature-time relationship (1% concrete)

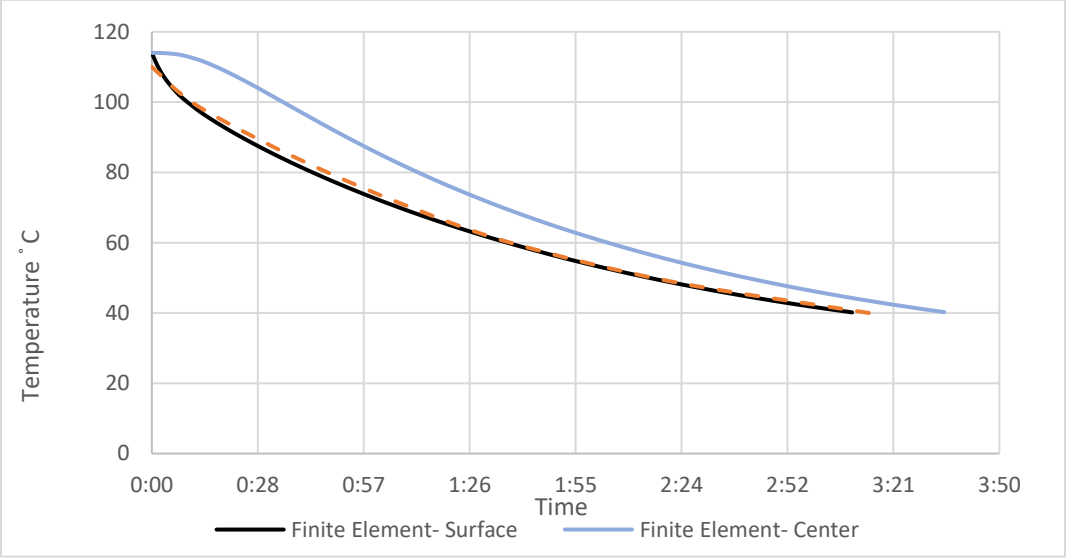

FIGURE 11 (c) Temperature-time relationship (2% concrete)

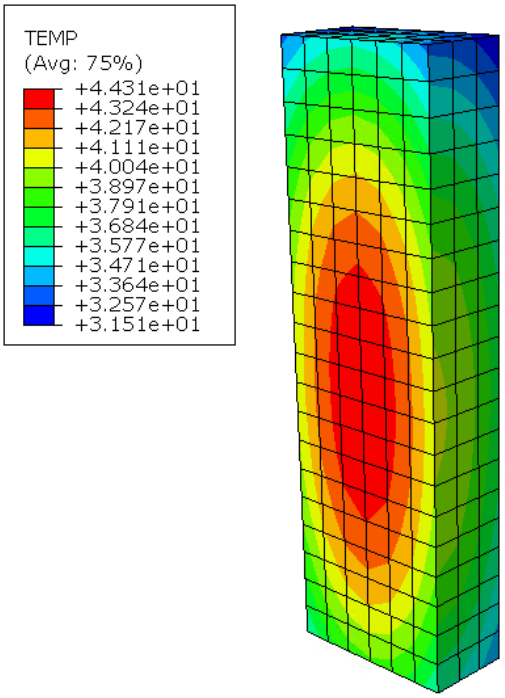

FIGURE 12 Inner section temperature

CONCLUSIONS

In this study, heated conductive concrete columns, made by adding waste steel shavings, was tested during cooling process to determine the self-sensing capabilities of the modified material. The experimental results showed that the technology is capable of quantifying the temperature changes of the concrete material and that the technique does not increase the specimen temperature during the introduction of electric currents. The lessons learned from this study are summarized as:

1) It was proven, using simple experimental setup, the detection capability of the effect of thermal changes on the conductive concrete.
2) For temperatures higher than 80°C, the electrical conductivity is directly proportional and highly sensitive to the temperature change and become less sensitive as the temperature decrease. This may be due to insignificant changes of the steel and concrete properties at lower temperatures.
3) The voltage and current readings are directly proportional to the temperature change. The concrete that contains steel shaving has less resistance to the current, which results in lower voltage values.
4) For self-sensing concrete purposes, at normal environmental temperature the small temperature changes will not have a critical effect on the voltage and current readings. But for applications that require high-temperature exposure, the concrete temperature becomes critical in assisting the self-sensing concrete condition.
5) The heat generated by the 25.5 V applied to the specimen can be ignored.

6) From the finite element model, the surface temperatures have little contribution with the temperature at the exposed electrodes when they are located at less than 75 mm from the surface and can be used in the analysis.

REFERENCES

ACI 211 (2014) “Standard Practice for Selecting Proportions for Normal, Heavyweight, and Mass Concrete,” American Concrete Institute, ACI 211.5R-14.

ACI 544 (2018) “Guide to Design with Fiber-Reinforced Concrete,” American Concrete Institute, ACI 544.4R.

ASCE (2017), US Infrastructure Report Card, American Society of Civil Engineers, Reston, VA.

Scott, D. (2018) “Evaluation of Discrete Sensing Materials in Concrete Using Recycled and Graded Steel Shavings” PhD Dissertation, Department of Civil and Environmental Engineering, University of North Carolina at Charlotte, Charlotte, NC.

Wu, T., Huang, R., Chi, M. and Weng, T. (2013) “A Study on Electrical and Thermal Properties of Conductive Concrete” Computers and Concrete, 12(3), 337-349.

Tuan, C.Y. (2004) “Conductive Concrete for Bridge Deck Deicing” Concrete Technology Today, Portland Cement Association (PCA), 25(1), CT041, 2 pages.

Chrisp, T.M., Starrs, G., McCarter, W.J., Rouchotas, E. and Elewett, J. (2001) “Temperature-Conductivity Relationships for Concrete: An Activation Energy Approach” Journal of Materials Science Letters, 20, 1085-1087.

Eurocode 2: Design of Concrete Structures (EN 1992-1-2 2004)

Ou, J. and Han, B. (2009) “Piezoresistive Cement-based Strain Sensors and Self-sensing Concrete Components” Journal of Intelligent Material Systems and Structures, 20, 329-336.

Wen, S. and Chung, D.D.L. (2007) “Electrical Resistance-Based Damage Self-Sensing in Carbon Fiber Reinforced Cement” Carbon, 45(4), 710-716.

Chung, D.D.L. (2002). “Electrical Conduction Behavior of Cement-Matrix Composites,” Journal of Materials Engineering and Performance, 11(2), 194-204.

Azhari, F., Banthia, N. (2012) “Cement-Based Sensors with Carbon Fibers and Carbon Nanotubes for Piezoresistive Sensing” Cement and Concrete Composites, 34(7), 866-873.

Ramli, M. and Dawood, E.T. (2011) “Effect of Steel Fibers on the Engineering Performance of Concrete” Asian Journal of Applied Sciences, 4(1), 97-100.

Yehia, S., Tuan, C.Y., Ferdon, D. and Chen, B. (2000) “Conductive Concrete Overlay for Bridge Deck Deicing: Mixture Proportioning, Optimization, and Properties” ACI Materials Journal, 97(2), 172-181.

Yehia, S.A. and Tuan, C.Y. (2000), “Thin Conductive Concrete Overlay for Bridge Deck Deicing and Anti-Icing”, Transport. Res. Rec., 1698, 45-53.

Yehia, S. and Tuan, C.Y. (2002), “Conductive Concrete Overlay-An Innovative Solution for Bridge Deck Deicing”, Concrete International, 24, 56-60.

Yehia, S. (2008), “Electrically Conductive Concrete Proves Effective as Bridge Deicer”, Road Bridge, 46, 32-35.

Videla, C.C., Covarrubias, J.P.T. and Pascual, J.M.D. (1996) “Behaviour in Extreme Climates of Concrete Made with Different Types of Cement” Concrete in the Service of Mankind: Appropriate Concrete Technology, Vol. 3, Dhir, R.K. and McCarthy, M.J. edit, E &FN, London, U.K. ISBN 0419214704, 209-222.

Samarin, A. (2013) "Use of Concrete as a Biological Shield from Ionising Radiation." Energy and Environmental Engineering, 1.2, 90 – 97.

Mortazavi, S.M.J., Mosleh-Shirazi, M.A., Baradaran-Ghahfarokhi, M., Siavashpour, Z., Farshadi, A., Ghafoori, M. and Shahvar, A. (2010) “Production of a Datolite-Based Heavy Concrete for Shielding Nuclear Reactors and Megavoltage Radiotherapy Rooms Production of a Datolite-Based Heavy Concrete” Iranian Journal of Radiation Research, 8(1), 11-15.

Qasrawi, H., Shalabi, F. and Asi, I. (2009) “Use of Low Cao Unprocessed Steel Slag in Concrete as Fine Aggregate” Construction and Building Materials, 23, 1118-1125.

Han B., Yu X., and Ou J. (2014). Self-Sensing Concrete in Smart Structures, Elsevier Inc., Oxford, UK.

Guo, L.X., Guo, L., Zhong, L. and Zhu, Y.M. (2011) “Thermal Conductivity and Heat Transfer Coefficient of Concrete” Journal of Wuhan University of Technology-Mater Sci. Ed., 2011, 791-796 .

Rajabipour (2006) Insitu Electrical Sensing and Material Health Monitoring in Concrete Structures, Ph.D. Dissertation, Department of Civil Engineering, Purdue University, Lafayette, IN.

Pace, J. (2016) “Disposal Processes of Steel Shaving” Personal Communication.

Xie, P., Gu, P. and Beaudoin, J.J. (1996) “Electrical Percolation Phenomena in Cement Composites Containing Conductive Fibres,” Jounral of Material Science, 31, 4093 - 4097.